

## UPPER LIMITS ON THE CONTINUUM EMISSION FROM GEMINGA AT 74 AND 326 MHz

NAMIR E. KASSIM AND T. JOSEPH W. LAZIO

Naval Research Laboratory, Code 7213, Washington, DC 20375-5351;

kassim@rsd.nrl.navy.mil, lazio@rsd.nrl.navy.mil

Received 1999 September 13; accepted 1999 October 20; published 1999 November 29

### ABSTRACT

We report a search for radio continuum emission from the gamma-ray pulsar Geminga. We have used the VLA to image the location of the optical counterpart of Geminga at 74 and 326 MHz. We detect no radio counterpart. We derive upper limits to the pulse-averaged flux density of Geminga, taking diffractive scintillation into account. We find that diffractive scintillation is probably quenched at 74 MHz and does not influence our upper limit,  $S < 56$  mJy ( $2\sigma$ ), but that a 95% confidence level at 326 MHz is  $S < 5$  mJy. Owing to uncertainties on the other low-frequency detections and the possibility of intrinsic variability or extrinsic variability (refractive interstellar scintillation) or both, our nondetections are nominally consistent with these previous detections.

*Subject headings:* pulsars: individual (Geminga) — radio continuum: stars

### 1. INTRODUCTION

The gamma-ray pulsar Geminga (PSR J0633+1746, 1E 0630+178, ICG 195+04) was first identified as a compact gamma-ray source in the Galactic anticenter (Hermsen et al. 1977; Thompson et al. 1977). Although initial speculation included the possibility that this source was a pulsar, its identification as such was not secure until the detection of X-ray pulsations (Halpern & Holt 1992; Bertsch et al. 1992). Since pulsars are typically bright in the radio portion of the spectrum, intense effort has been devoted to finding a radio counterpart to Geminga (Table 1).

Until recently, only upper limits on the radio emission from Geminga could be established. However, a number of groups have now reported detecting pulsed radio emission from Geminga near 100 MHz (Kuz'min & Losovskii 1997a, 1997b; Malofeev & Malov 1997; Shitov et al. 1997; Shitov & Pugachev 1997; Vats et al. 1997, 1999). However, subsequent attempts to detect pulsed emission at frequencies of 35 and 326 MHz have failed (Ramachandran, Deshpande, & Indrani 1998; McLaughlin et al. 1999). In an effort to constrain further the radio spectrum of Geminga, we have conducted 74 and 326 MHz observations of it. In § 2 we describe our observations, in § 3 we obtain upper limits for the Geminga pulsar that take interstellar scintillation into account, and in § 4 we discuss our results.

### 2. OBSERVATIONS

Reported previous detections of Geminga have been in the range 41–103 MHz (Table 1). Subsequent attempts to confirm these detections have been close to, but outside of, this frequency range. The nondetection at 35 MHz (Ramachandran et al. 1998) seems problematic, but a combination of a low-frequency cutoff in the spectrum and interstellar scintillation may explain the detection at 41 MHz and the upper limit at 35 MHz. The observations reported here are significant in that they are the only attempt to confirm the radio emission from Geminga within the frequency range of the reported detections.

Our observations were conducted on 1998 March 9 with the VLA in the A configuration; Table 2 summarizes various details. Ionospheric phase variations would have vitiated a periodicity search, so our observations were designed to image only the pulse-averaged emission from the pulsar. The various

detections suggest that the radio pulse is extremely wide, covering perhaps  $90^\circ$  of pulse phase. Thus, our attempt to detect Geminga should not be affected significantly by searching for a point source at its location.

Postprocessing of low-frequency VLA data uses procedures similar to those at higher frequencies, although certain details differ.<sup>1</sup> At 74 MHz Cygnus A served as both the flux density and visibility phase calibrator. At 326 MHz the primary flux density calibrator was 3C 48, whose flux density was taken to be 52.2 Jy, and phase calibration was accomplished with frequent observations of 4C 14.18. At both frequencies, after initial phase calibration, several iterations of hybrid mapping were used to improve the dynamic range.

Two significant differences for the postprocessing were the impact of radio frequency interference (RFI) and the large fields of view. In order to combat RFI, the data were acquired with a much higher spectral resolution than used for imaging. Excision of potential RFI is performed on a per-baseline basis for each 10 s visibility spectrum. The large fields of view ( $11^\circ$  at 74 MHz,  $2.5^\circ$  at 326 MHz) mean that the sky cannot be approximated as flat. In order to approach the thermal noise limit, we used a polyhedron algorithm (Cornwell & Perley 1992) in which the sky is approximated by many two-dimensional “facets.”

We did not image the data at the same spectral resolution with which they were acquired. Sources in our images are identified on the basis of their brightness. Bandwidth smearing can cause weak sources in the outer portions of the primary beam to have a brightness below our detection threshold. The sidelobes of any such undetected sources contribute to the noise in the image. Increasing the spectral resolution has the beneficial result of decreasing the amount of bandwidth smearing; however, it also increases the computational expense and the impact of diffractive scintillation. In fact, for reasonable choices of the scintillation properties for the line of sight toward Geminga (§ 3), the impact of diffractive scintillation will be unchanged for the range of spectral resolutions we have available. The primary factors for deciding the spectral resolution are the desire to minimize bandwidth smearing versus computational expense. The bandwidths we used—122 kHz at 74 MHz and

<sup>1</sup> A full description of low-frequency VLA data reduction procedures is at <http://rsd-www.nrl.navy.mil/7213/lazio/tutorial>.

Report Documentation Page			Form Approved OMB No. 0704-0188		
Public reporting burden for the collection of information is estimated to average 1 hour per response, including the time for reviewing instructions, searching existing data sources, gathering and maintaining the data needed, and completing and reviewing the collection of information. Send comments regarding this burden estimate or any other aspect of this collection of information, including suggestions for reducing this burden, to Washington Headquarters Services, Directorate for Information Operations and Reports, 1215 Jefferson Davis Highway, Suite 1204, Arlington VA 22202-4302. Respondents should be aware that notwithstanding any other provision of law, no person shall be subject to a penalty for failing to comply with a collection of information if it does not display a currently valid OMB control number.					
1. REPORT DATE <b>DEC 1999</b>		2. REPORT TYPE		3. DATES COVERED <b>00-00-1999 to 00-00-1999</b>	
4. TITLE AND SUBTITLE <b>Upper Limits on the Continuum Emission from Geminga at 74 and 326 MHz</b>			5a. CONTRACT NUMBER		
			5b. GRANT NUMBER		
			5c. PROGRAM ELEMENT NUMBER		
6. AUTHOR(S)			5d. PROJECT NUMBER		
			5e. TASK NUMBER		
			5f. WORK UNIT NUMBER		
7. PERFORMING ORGANIZATION NAME(S) AND ADDRESS(ES) <b>Naval Research Laboratory, Code 7213, 4555 Overlook Avenue, SW, Washington, DC, 20375</b>			8. PERFORMING ORGANIZATION REPORT NUMBER		
9. SPONSORING/MONITORING AGENCY NAME(S) AND ADDRESS(ES)			10. SPONSOR/MONITOR'S ACRONYM(S)		
			11. SPONSOR/MONITOR'S REPORT NUMBER(S)		
12. DISTRIBUTION/AVAILABILITY STATEMENT <b>Approved for public release; distribution unlimited</b>					
13. SUPPLEMENTARY NOTES					
14. ABSTRACT					
15. SUBJECT TERMS					
16. SECURITY CLASSIFICATION OF:			17. LIMITATION OF ABSTRACT	18. NUMBER OF PAGES <b>4</b>	19a. NAME OF RESPONSIBLE PERSON
a. REPORT <b>unclassified</b>	b. ABSTRACT <b>unclassified</b>	c. THIS PAGE <b>unclassified</b>			

TABLE 1  
OBSERVATIONAL LIMITS ON THE RADIO COUNTERPART  
OF GEMINGA BELOW 1000 MHz

Frequency (MHz)	Flux Density (mJy)	Reference
Periodicity Searches		
35 .....	<100	1
41 .....	300	2
61 .....	111	2
102 .....	<100	3
102.5 .....	60 ± 95	4
	(5–500)	...
	8 <sup>+3</sup> <sub>-2</sub>	5
103 .....	1000	6
318 .....	<1	7
	<3.1	8
	<0.1	9
325 .....	<2500	10
327 .....	<0.3	1
	<3	11
430 .....	<1	7
	<0.6	8
	<0.05	9
928 .....	<6	12
Continuum Searches		
74 .....	<56	13
326 .....	<5.0	13

NOTE.—Only the work of McLaughlin et al. 1999 and that reported here have taken interstellar scintillation into account explicitly in setting upper limits.

REFERENCES.—(1) Ramachandran et al. 1998; (2) Shitov et al. 1997; (3) Kuz'min & Losovskii 1997b; (4) Malofeev & Malov 1997; (5) Shitov & Pugachev 1997; (6) Vats et al. 1999; (7) D'Amico 1983; (8) Fauci, Boriakoff, & Buccheri 1984; (9) Buder, Fauci, & Boriakoff 1999; (10) Mandolesi, Morigi, & Sironi 1978; (11) McLaughlin et al. 1999; (12) Seiradakis 1981; (13) this work.

684 kHz at 326 MHz—gave modest spectral resolutions (a few), modest bandwidth smearing near the edge of the primary beam (~10%), and reasonable imaging times (less than a few days of computation).

Figure 1 shows our 74 MHz image of the immediate region around Geminga. The off-source rms noise level on this image is 28 mJy beam<sup>-1</sup>, and the estimated thermal limit is 25 mJy beam<sup>-1</sup>. Figure 2 shows our 326 MHz image of the immediate region around Geminga. The off-source rms noise level on this image is 1.4 mJy beam<sup>-1</sup>, and the estimated thermal limit is 0.5 mJy beam<sup>-1</sup>.

One additional impact on the 74 MHz observations is ionospheric refraction, which shifts the field of view without distorting the brightness distribution (Erickson 1984). Shifts at 74 MHz are typically a few arcminutes and vary on timescales of tens of minutes. Self-calibration “freezes” out this refraction but destroys absolute position information. Fortunately, the primary beam is large enough that a typical image contains many tens of sources identified in the 1400 MHz NRAO VLA Sky Survey (NVSS; Condon et al. 1998). We constructed a reference grid using 42 NVSS sources that were either unresolved or slightly resolved (diameters less than 30"). In determining the reference grid, we checked for any systematic trends as a function of position within the 74 MHz image, flux densities of the sources, or angular diameters of the sources. None were found. We shifted the 74 MHz image by the median offsets, 3".9 in right ascension and -58".4 in declination. Based on the variances of the offsets from the reference sources, our 74 MHz

TABLE 2  
VLA OBSERVING LOG

$\nu$ (MHz)	$B$ (MHz)	$B_i$ (kHz)	$T$ (hr)	Beam (arcsec)	$\Delta I$ (mJy beam <sup>-1</sup> )	$F$ (mJy)
74 .....	1.5	122	5.4	25 × 23 at 64°	28	-13
326 .....	3	684	5.4	5.1 × 4.8 at 75°	1.4	0.28

NOTE.— $B$  is the total observing bandwidth, while  $B_i$  is the bandwidth used in imaging.  $T$  is the on-source integration time.  $\Delta I$  is the rms noise level in the image, and  $F$  is the measured flux density at the location of Geminga.

astrometry should be accurate to approximately 5", a fraction of the beam diameter, for an individual source. Figure 1 has been corrected for refraction.

### 3. UPPER LIMITS AND INTERSTELLAR SCINTILLATION

In this section we address our upper limits on Geminga's flux density and the impact of scintillation on them. We shall follow the procedure described by McLaughlin et al. (1999) for dealing with the effects of interstellar scintillation (ISS).

Briefly, their procedure involves convolving the known probability density functions (pdf's) for the diffractive ISS gain and noise in the image to produce a pdf for the measured flux density for the scintillating source. This pdf is then multiplied by a *prior* for the intrinsic flux density of the source (Geminga) to form the *posterior* for the intrinsic flux density of the source. Since our images were constructed using an fast Fourier transform, without specifying a zero-spacing flux density, we have assumed (and verified) that the noise in the image has a zero-mean Gaussian pdf.

In addition to the rms noise in the image (Table 2), we require two additional parameters: a measure of the strength of diffractive ISS (DISS) and a measured flux density at the location of Geminga. The former is provided by  $N_{\text{DISS}}$ , the number of

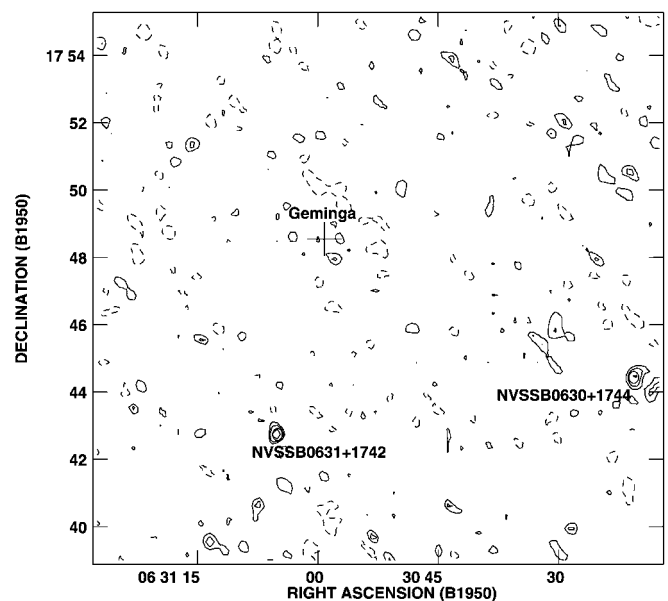


FIG. 1.—Geminga field at 74 MHz. The cross marks the location of the optical counterpart of Geminga (Caraveo et al. 1998); the uncertainty in the location of Geminga is approximately 100 times smaller than the size of the cross. The beam is 24".6 × 23".3 at a position angle of 64°, and the rms noise level is 28 mJy beam<sup>-1</sup>. Contour levels are 28 mJy beam<sup>-1</sup> × -2, 2, 3, 5. Also indicated are two sources from the NRAO VLA Sky Survey (Condon et al. 1998).

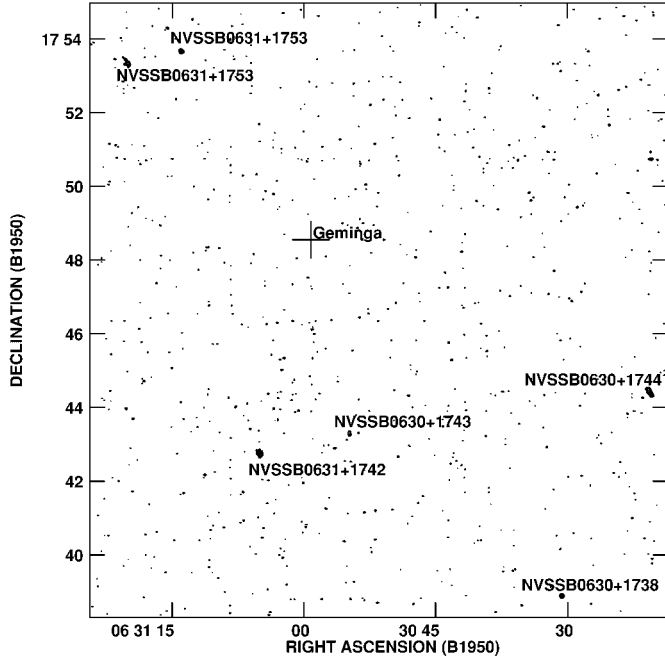


FIG. 2.—Geminga field at 326 MHz. A cross marks the location of the optical counterpart of Geminga (Caraveo et al. 1998); the uncertainty in the location of Geminga is approximately 100 times smaller than the size of the cross. The beam is  $5''.0 \times 4''.8$  at a position angle of  $75^\circ$ , and the rms noise level is  $1.4 \text{ mJy beam}^{-1}$ . Contour levels are  $1.4 \text{ mJy beam}^{-1} \times -3, 3, 5, 7.07, 10, 14.1, \dots$ . Also indicated are a number of sources from the NRAO VLA Sky Survey (Condon et al. 1998).

“scintilles” or scintillation intensity maxima occurring during the entire observation (Cordes 1986; McLaughlin et al. 1999). For Geminga, there are no published measurements of the relevant ISS parameters, the scintillation time  $\Delta t_d$  or the scintillation bandwidth  $\Delta \nu_d$ . McLaughlin et al. (1999) estimated these parameters to be  $\Delta t_d \approx 275 \text{ s} (\nu/327 \text{ MHz})^{-2.2}$  and  $\Delta \nu_d \approx 1.5 \text{ MHz} (\nu/327 \text{ MHz})^{4.4}$ . Their values imply a scattering measure toward Geminga of  $\text{SM} \sim 10^{-4.4} \text{ kpc m}^{-20/3}$ . While consistent with the local distribution of scattering material, there are also large variations in the value of SM for pulsars at distances comparable to that of Geminga: PSR J0437–4715 with  $D = 0.18 \text{ kpc}$  and  $\text{SM} = 10^{-3.8} \text{ kpc m}^{-20/3}$  (Sandhu et al. 1997; Johnston, Nicastro, & Koribalski 1998) versus PSR B0950+08 with  $D = 0.125 \text{ kpc}$  and  $\text{SM} = 10^{-4.5} \text{ kpc m}^{-20/3}$  (Gwinn et al. 1986; Phillips & Clegg 1992). We shall adopt McLaughlin et al.’s (1999) value for SM but note how a different value affects our results. For our integration time and receiver bandwidth, the resulting values are  $N_{\text{DISS}} = 910$  at 74 MHz and  $N_{\text{DISS}} = 15$  at 326 MHz.

We obtain the flux density at the location of Geminga by integrating over an area of 1 beam at the position of Geminga. We use the term “flux density at the location of Geminga” because of the noise in the image. Since the noise is zero-mean, there are both positive and negative intensity variations. A weak source combined with a large negative noise deviation could result in a measured flux density quite different than that of the intrinsic flux density of the source. Given the sizes of the beams ( $6''$  at 326 MHz and  $25''$  at 74 MHz), this integration also takes into account the uncertainty in the position of Geminga, which is less than  $1''$  (Bignami, Caraveo, & Mereghetti 1993; Caraveo et al. 1996).

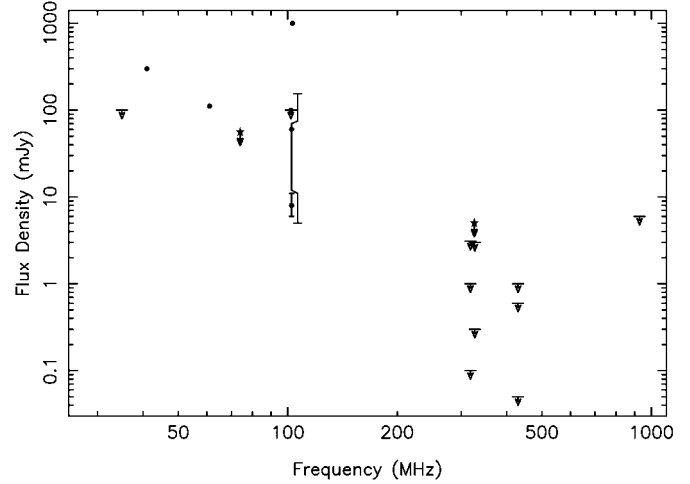


FIG. 3.—Radio spectrum of Geminga below 1000 MHz. The upper limits reported in this Letter are marked with a star. Limits and detections are summarized in Table 1. With the exception of the upper limit by McLaughlin et al. (1999;  $<3 \text{ mJy}$  at 326 MHz), all other upper limits have not considered the effects of interstellar scintillation.

### 3.1. 74 MHz

We begin by determining the upper limit on Geminga’s flux density if ISS was not an issue. The position of Geminga’s optical counterpart, even taking into account its proper motion, is known to accuracy far better than the beam diameter of  $25''$ . We therefore adopt an upper limit of 56 mJy, twice the rms noise level.

As  $N_{\text{DISS}} \rightarrow \infty$ , DISS becomes more and more heavily quenched, and the pdf of the DISS gain approaches a  $\delta$ -function centered on unity. We consider  $N_{\text{DISS}} \sim 10^3$  sufficiently large that DISS will not affect our upper limit. If our adopted value of SM were too large and the correct value were  $\text{SM} \sim 10^{-5.3} \text{ kpc m}^{-20/3}$ —comparable to that for PSR B0950+08—then  $N_{\text{DISS}} = 44$ . We would obtain an upper limit for Geminga’s flux density of  $S < 86 \text{ mJy}$  at the 95% confidence level.

### 3.2. 326 MHz

If we ignore ISS, the  $6''$  beam remains large enough that we adopt an upper limit of 2.8 mJy, again twice the rms noise level.

Our adopted value of SM implies  $N_{\text{DISS}} = 15$ . In contrast to the situation at 74 MHz, DISS can have a substantial impact on the adopted flux density at 326 MHz. We find an upper limit on Geminga’s flux density of  $S < 5.0 \text{ mJy}$  at the 95% confidence level. If our adopted value of SM were too large, and the correct value were  $\text{SM} \sim 10^{-5.3} \text{ kpc m}^{-20/3}$ , then  $N_{\text{DISS}} = 5$ . We would obtain an upper limit for Geminga’s flux density of  $S < 13.5 \text{ mJy}$  at the 95% confidence level.

## 4. CONCLUSIONS

Figure 3 incorporates our upper limits with the limits and detections of Geminga below 1000 MHz in the literature; Table 1 summarizes the data shown in Figure 3.

Can we reconcile our nondetection with the detections near 100 MHz? One simple possibility is that the pulse-averaged radio emission from Geminga is intrinsically time variable. In this case, our nondetection is quite easy to reconcile with the

various detections. Vats et al. (1999) argue that Geminga is intrinsically time variable in order to explain their detection with a flux density of 1 Jy at 103 MHz, and they speculate on intrinsic mechanisms that could be responsible.

Even if we treat the Vats et al. (1999) detection at 103 MHz as an outlier, though, our nondetection is just consistent with the other detections near 100 MHz. Shitov & Pugachev (1997) report a flux density of  $8_{-2}^{+3}$  mJy at 102.5 MHz. Clearly, if this is the intrinsic flux density, then there is no difficulty reconciling this with our nondetection.

There are two difficulties with assuming a flux density of 8 mJy at 102 MHz, though. First, it requires Geminga to have an extremely steep spectrum between 61 and 102 MHz,  $\alpha \approx -5$ , although Geminga's radio emission mechanism might be different than that of other pulsars. Second, it is difficult to explain other detections at 102 MHz. Some combination of intrinsic and ISS-induced intensity variation could in principle explain this dynamic range, but in practice it might require improbably large DISS gains.

A more likely value for the 100 MHz flux density is near 50 mJy, in which case Shitov & Pugachev (1997) detected it in an ISS-depressed state. This explanation is appealing in two respects. First, a DISS gain of 0.1 would depress the flux density from near 50 mJy to near 5 mJy, and a DISS gain this small has a probability of occurrence near 90%. Second, the spectral index between 61 and 102 MHz would be  $-1.6$ , more characteristic of radio pulsars. In this case, the expected flux density at 74 MHz is 80 mJy, above our upper limit for our nominal value of  $N_{\text{DISS}}$ , but below it if our adopted value of SM is too large.

In reconciling our nondetection at 74 MHz with the detections, we have relied on the robustness of the 41 and 61 MHz observations. In reporting their detections at these frequencies, Shitov et al. (1997) did not indicate to what extent DISS had been quenched. Since DISS is more likely to depress than to enhance the flux density of a source, the 41 and 61 MHz

detections could represent *lower* limits to Geminga's flux density. If so, reconciliation would be more difficult.

One aspect of ISS not addressed quantitatively is the impact of *refractive* ISS (RISS). At low frequencies, ISS has an anticipatory nature: DISS occurring on "short" timescales and RISS occurring on "long" timescales. RISS is more difficult to quench than DISS because its timescales are typically hours to days, so the flux density of Geminga could be enhanced or suppressed for an entire observing run. RISS could serve as the extrinsic mechanism that would contribute both to our nondetection (and that of Ramachandran et al. 1998 at 35 MHz) and the detections near 100 MHz.

RISS is more difficult to handle quantitatively because its pdf is not as well constrained as the pdf for DISS. Some indication of the effect of RISS can be obtained by adopting a lognormal pdf (Ishimaru 1978, chap. 20). Gupta, Rickett, & Coles (1993) found a refractive intensity modulation variance  $m_r^2 \approx 0.2$  for PSR B0950+08 at 74 MHz. This variance, when used with a lognormal pdf, implies a (95% probability) range of RISS-induced variations of a factor of a few. Thus, these low-frequency measurements and upper limits could have an additional factor of 2 or so uncertainty.

In summary, we have not detected Geminga at 74 MHz ( $S < 56$  mJy) or 326 MHz ( $S < 5$  mJy). We can reconcile our nondetection with previous low-frequency detections by invoking intrinsic variability or extrinsic variability (refractive interstellar scintillation) or both.

This research made use of NASA's ADS Abstract Service and the SIMBAD database, operated at the CDS, Strasbourg, France. The National Radio Astronomy Observatory is a facility of the National Science Foundation operated under cooperative agreement by Associated Universities, Inc. The results presented here made use of the Department of Defense High Performance Computing Modernization Program. Basic research in radio astronomy at the NRL is supported by the Office of Naval Research.

#### REFERENCES

- Bertsch, D. L., et al. 1992, *Nature*, 357, 306  
 Bignami, G. F., Caraveo, P. A., & Mereghetti, S. 1993, *Nature*, 361, 740  
 Burderi, L., Fauci, F., & Boriakoff, V. 1999, *ApJ*, 512, L59  
 Caraveo, P., Bignami, G., Mignani, R., & Taff, L. G. 1996, *ApJ*, 461, L91  
 Caraveo, P. A., Lattanzi, M. G., Massone, G., Mignani, R. P., Makarov, V. V., Perryman, M. A. C., & Bignami, G. F. 1998, *A&A*, 329, L1  
 Condon, J. J., Cotton, W. D., Greisen, E. W., Yin, Q. F., Perley, R. A., Taylor, G. B., & Broderick, J. J. 1998, *AJ*, 115, 1693  
 Cordes, J. M. 1986, *ApJ*, 311, 183  
 Cornwell, T. J., & Perley, R. A. 1992, *A&A*, 261, 353  
 D'Amico, N. 1983, *Space Sci. Rev.*, 36, 195  
 Erickson, W. C. 1984, *J. Astrophys. Astron.*, 5, 55  
 Fauci, F., Boriakoff, V., & Buccheri, R. 1984, *Nuovo Cimento*, 7C, 597  
 Gupta, Y., Rickett, B. J., & Coles, W. A. 1993, *ApJ*, 403, 183  
 Gwinn, C. R., Taylor, J. H., Weisberg, J. M., & Rawley, L. A. 1986, *AJ*, 91, 338  
 Halpern, J. P., & Holt, S. S. 1992, *Nature*, 357, 222  
 Hermesen, W., et al. 1977, *Nature*, 269, 494  
 Ishimaru, A. 1978, *Wave Propagation and Scattering in Random Media* (Boston: Academic)  
 Johnston, S., Nicastro, L., & Koribalski, B. 1998, *MNRAS*, 297, 108  
 Kuz'min, A. D., & Losovskii, B. Ya. 1997a, *IAU Circ.* 6559  
 ———. 1997b, *Pisma Astron. Zh.*, 23, 323 (transl. *Astron. Lett.*, 23, 283)  
 Malofeev, V. M., & Malov, O. I. 1997, *Nature*, 389, 697  
 Mandolesi, N., Morigi, G., & Sironi, G. 1978, *A&A*, 67, L5  
 McLaughlin, M. A., Cordes, J. M., Hankins, T. H., & Moffett, D. A. 1999, *ApJ*, 512, 929  
 Phillips, J. A., & Clegg, A. W. 1992, *Nature*, 360, 137  
 Ramachandran, R., Deshpande, A. A., & Indrani, C. 1998, *A&A*, 339, 787  
 Sandhu, J. S., Bailes, M., Manchester, R. N., Navarro, J., Kulkarni, S. R., & Anderson, S. B. 1997, *ApJ*, 478, L95  
 Seiradakis, J. H. 1981, *A&A*, 101, 158  
 Shitov, Yu. P., Malofeev, V. M., Malov, O. I., & Pugachev, V. D. 1997, *IAU Circ.* 6775  
 Shitov, Yu. P., & Pugachev, V. D. 1997, *NewA*, 3, 101  
 Thompson, D. J., Fichtel, C. E., Hartman, R. C., Kniffen, D. A., & Lamb, R. C. 1977, *ApJ*, 213, 252  
 Vats, H. O., Deshpande, M. R., Shah C., Singal, A. K., Iyer, K. N., Oza, R., & Doshi, S. 1997, *IAU Circ.* 6699  
 Vats, H. O., Singal, A. K., Deshpande, M. R., Iyer, K. N., Oza, R., Shah, C. R., & Doshi, S. 1999, *MNRAS*, 302, L65